Pergamon

Tetrahedron Vol. 51, No. 2, pp. 607-619, 1995

0040-4020/95 $9.50+0.00

0040-4020(94)00920-1

Design and Synthesis of Hydrogen-bonded Aggregates. Theory and Computation Applied to Three Systems Based on the Cyanuric Acid-Melamine Lattice[1]

Eric E. Simanek, Mathai Mammen, Dana M. Gordon, Donovan Chin,
John P. Mathias, Christopher T. Seto, and George M. Whitesides*

Department of Chemistry, Harvard University
Cambridge, MA 02138

Abstract

The rational design of complex, self-assembling, non-covalent aggregates requires a workable understanding of association phenomena, a reliable rule-based mechanism to predict and compare the stabilities of potential target structures, and straightforward synthetic routes to the molecular components of the aggregates. Systems based on the cyanuric acid-melamine lattice satisfy many of these criteria. This paper reviews the design, synthesis, and characterization of three related aggregates, and summarizes initial results of two models: i) a computational model that predicts relative stabilities of aggregates; and ii) a theoretical model that assesses relative entropies of aggregation.

Introduction.

This paper describes: i) the synthesis and characterization of three experimental systems based on networks of hydrogen bonds; ii) the application of a simple model to address the theoretical bases that govern non-covalent aggregation; and iii) the development of a computational model to aid in the design of these systems. The goal of our program is the rational design of non-covalent organic aggregates.

Hydrogen bonds are characterized by significant bond enthalpies, high directionality, and well-defined donor and acceptor groups. The substantial effort invested in understanding hydrogen bonding makes it one choice for the development of a rule-based system of self-assembly.[2] The cyclic hexamer (rosette) of the cyanuric acid-melamine (CA•M) lattice[3] (Figure 1) was selected as the basis for our systems because it has high symmetry, it generates a large number of hydrogen bonds, and the synthesis of its triazine components is straightforward.

The models used in this study are shown (in atomic detail and schematically) in Scheme 1. Each aggregate incorporates the rosette motif and is, therefore, held together by 18 hydrogen bonds. Aggregate **1** comprises six free monomers.[4] Both **2** and **3** are assemblies that comprise

four molecules; the three melamines are attached to a central hub by spokes.[5] Aggregates **2** and **3** differ in the constitution of their spokes: **2** incorporates a flexible 1,3-propanediol into the spoke while **3** utilizes a more rigid *m*-phenylenediamine. We refer to the trismelamine components of **2**

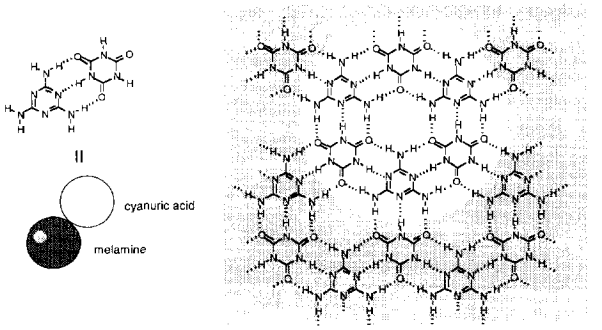

Figure 1. The lattice comprising cyanuric acid and melamine exists as an extended sheet (with 3HCl in the X-ray structure). We refer to the highlighted portion as the "rosette." This cyclic hexamer is held together by 18 hydrogen bonds and is the basis for all the structures based on hydrogen-bonding assemblies that we have reported to date. Melamines and isocyanuric acids are represented with darkened balls and white balls, respectively.

and **3** as flex(M)$_3$ and hub(M)$_3$, respectively. We characterized these aggregates by ^{1}H and ^{13}C NMR spectroscopies, gel permeation chromotography (GPC), vapor phase osmometry (VPO), and titration/solubilization experiments. These results and techniques are reviewed in the following sections. We recognized in the course of our studies that these aggregates have markedly different stabilities. This observation prompted us to develop theoretical and computational approaches to optimize the process of design of new aggregates.

Scheme 1. Schematic and atomic representations of **1**, **2**, and **3**. The relative rigidities of the spokes tethering melamines to a central hub in **2** and **3** are represented by wavy (flexible) and straight (rigid) lines, respectively. R= $CH_2CH_2C(CH_3)_3$. X=CEt_2. R'=*p*-*t*-BuPh. Y=NR.

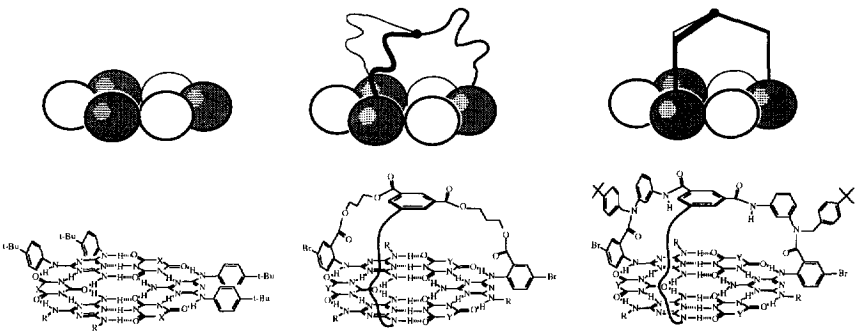

1 **2** **3**

Experiment

Scheme 2 outlines the syntheses of 1, 2, and 3. The sequential addition of amines to cyanuric chloride generates trisubstituted melamines.[6] Yields were typically high for this three-step, one-flask, 24 h reaction sequence. Reaction of nitrobiuret[7] with the desired aryl/alkyl amine yielded an intermediate biuret adduct. After isolation, the alkylbiuret adduct was allowed to react with a carbonyl source--typically carbonyldiimidazole or diethylcarbonate-- to generate the desired cyanuric acid.[8] The overall yield for this sequence was greater than 50%, and varied with the amine used. Barbiturates were prepared by the condensation of urea with the appropriately substituted diethyl malonates.[9] This sequence produced barbiturates in high yields; the crude products were purified through simple recrystallization. Many barbiturates are also commercially available.

Scheme 2. The syntheses of the components of **1**, **2**, and **3**.

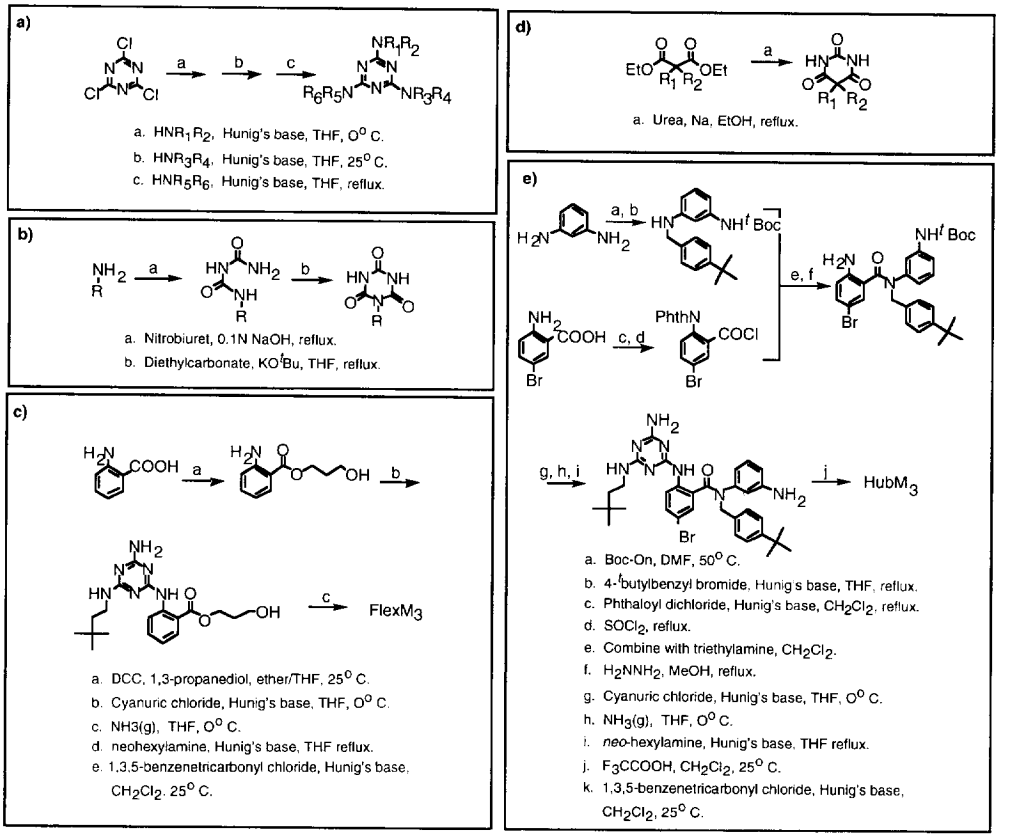

Titration/Solubilization. Monomeric derivatives of M or CA have low solubilities in organic solvents. Hub(M)$_3$ or flex(M)$_3$ are soluble in chloroform and most other organic solvents. Titration of CA into solutions (or for **1**, suspensions of M) indicates that the relative stoichiometries of melamine and cyanuric acid groups in these aggregates is 1: for **1**, M_3:CA_3; for **2**, flex(M)$_3$:3CA; for **3**, hub(M)$_3$:3CA. No significant amount of CA dissolves after three equivalents of it have been added to flex(M)$_3$ or hub(M)$_3$.

NMR Spectroscopy. The ^1H and ^{13}C NMR spectra of the uncomplexed trismelamine components of **2** and **3** in $CDCl_3$ are broad and featureless due to aggregation and slow interconversion of different conformations of these molecules. Sharp lines appear upon addition of CA. The intensity of these lines increases until three equivalents of CA have been added per equivalent of flex(M)$_3$ or hub(M)$_3$; the addition of more CA does not affect the intensity or shape of the lines. All lines of these spectra can be assigned. The assignment indicates that each spoke is in an indistinguishable environment.

Gel Permeation Chromatography (GPC). Gel permeation chromatography (GPC) is a size exclusion technique. The porous matrix allows small molecules to penetrate the stationary phase and causes them to remain on the column longer than larger molecules that are excluded from the stationary phase. GPC traces suggest the relative sizes and stabilities of aggregates: loss of components from an aggregate on the column is irreversible and can affect the shape of the GPC trace. For a covalent molecule like *p*-xylene, the peak is sharp lacking leading and trailing edges. We interpret the extent of trailing of a peak as being qualitatively inversely related to the stability of the aggregate. Figure 2 shows the GPC traces for **1**, **2**, and **3**.

Vapor Phase Osmometry (VPO). VPO provides an estimate of molecular weight; measurements are recorded as a voltage. This voltage reflects the amount of current required to heat a solution of known concentration of aggregate to maintain a temperature equivalent to pure solvent, while both are experiencing evaporative cooling. Comparing these voltages to the voltages recorded for solutions of an internal standard of similar mass provides a number-average molecular weight of the aggregate. These values are typically within 20% of the calculated weight of the aggregate. Figure 3 shows the VPO results for **1**, **2**, and **3**. We use four standards in order to obtain a estimate of the non-ideality of the standards, and to provide an estimate of the uncertainty in the MW values.

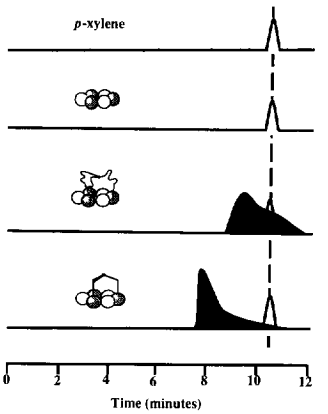

Figure 2. The GPC traces of *p*-xylenes, **1**+ *p*-xylenes (**1** is not stable to GPC), **2**+ *p*-xylenes, and **3**+ *p*-xylenes. The extent of tailing of these peaks is inversely proportional to the stabilities of the corresponding aggregate.

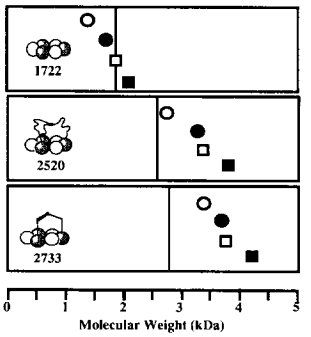

Figure 3. Molecular weights determined by VPO agree with the sum of the molecular weights expected based on the components to within 20%. Standards: (○) Gramacidin s (FW 1342); (●) sucrose octaacetate (FW 679); (□) polystyrene (FW 5050, polydispersity 1.05); (■) cyclodextrin (FW 3321).

Stability decreases in the order 3>2>1. The relative stabilities of these aggregates can be inferred from NMR competition experiments: aggregate **3** is more stable than **2** in chloroform. Three equivalents of *neo*-hexylCA form one aggregate, **3**, when dissolved in a solution containing hub$(M)_3$ and flex$(M)_3$. (When hub$(M)_3$ is mixed with **2**, aggregate **3** is formed leaving uncomplexed flex$(M)_3$ in solution. When flex$(M)_3$ is mixed with **3**, aggregate **3** remains leaving uncomplexed flex$(M)_3$ in solution). Upon addition of three more equivalents of *neo*-hexylCA,

both **2** and **3** are visible. Competition experiments between **2** or **3** and the components of **1** were unsuccessful. The ^{1}H NMR spectra of hub(M)$_3$ or flex(M)$_3$ with the melamine component of **1** with three equivalents of CA were complicated. Broadened resonances attributed to an undefined aggregate(s) were observed. We believe that the limited solubility of the components of **1** necessitates association with the soluble components of **2** or **3**, and make this experiment difficult to interpret.

Aggregate **1** is less stable than **2** or **3**. Evidence to support this assertion comes from the concentration dependence of the stability of **1** (and lack of a concentration dependence for **2** or **3**) as observed by ^{1}H NMR. We found that **1** is stable only at concentrations greater than >4 mM. Aggregates **2** and **3** are stable at <1 mM.

We can infer relative stabilities of these aggregates from the shape of the GPC traces. Dissociation of the aggregate on the GPC column leads to tailing of the peak. Stable aggregates show sharp peaks, while tailing peaks suggest less stable aggregates. The GPC trace of **3** shows less tailing than the trace of **2**, and is consistent with the observation that **3** is more stable than **2**. Aggregate **1** does not show a peak by GPC. We infer that aggregate **1** dissociates over the course of the experiment. The differences in stabilities by GPC suggests that stability of the aggregates decreases in the order **3>2>1**.

The Theoretical Basis for the Design of Non-covalent Aggregates.

The role of entropy can be addressed qualitatively with a simple model system: balls and strings. The thermodynamic stability of any non-covalent assembly is a balance of entropy and enthalpy. The enthalpy of association can be maximized by increasing the number of favorable enthalpic interactions between molecules. These interactions include hydrogen bonds, and hydrophobic, ionic, and polar interactions. Hydrogen bonds are strong (1-5 kcal/mol) and relatively directional with specific donor-acceptor roles; they are, therefore, a well-defined system for the examination of the roles of entropy and enthalpy in non-covalent assemblies. Each of the aggregates **1** - **3** forms 18 hydrogen bonds. If we assume a common enthalpic contribution to the free energy, then we have an opportunity to examine the role of entropy in these aggregates. The total entropic cost of bringing six recognition domains together to form one well-defined assembly can be discussed in terms of the components of entropy: translational, rotational, and conformational (vibrational). The different structures of the aggregates under consideration offer a starting point for the examination of these three entropic terms.

Translational entropy, S_{trans}, reflects the freedom of motion of a particle--the "ball"--in space. Under standard conditions, S_{trans} is a function of the logarithm of the molecular weight, ln(MW). The translational entropy of a single ball in solution, at concentration of 1 M, can be approximated

$$TS_{trans} = 3 + \ln(MW) \qquad \text{(eq 1)}$$

(in kcal/mol) at 300 K with equation 1.[10] Bringing N particles together to form a single aggregate occurs at great entropic cost: N-1 particles lose their initial translational entropy. This change in entropy can be estimated (in kcal/mol) using equation 2 (for balls of MW = 300 at T = 300 K; forming an aggregate at 1 M concentration from components at 1 M concentration). Covalently

$$T\Delta S_{trans} = 8(N-1) \qquad \text{(eq 2)}$$

stringing two or more balls together significantly reduces the magnitude of this loss of translational entropy. Table I includes approximate values of $T\Delta S_{trans}$ for **1**, **2**, and **3**. Aggregation of components to yield **2** and **3** requires that four particles form one aggregate: that is, that N-1 = 3 particles lose their initial translational entropy. Aggregation to form **1** requires that N-1 = 5 particles lose their initial translational entropy. As a result of the difference in losses of translational entropy, aggregation of four molecules is favored over aggregation of six molecules.

Table I. Approximate Entropic Contributions to Aggregation.[a]

Complex	$T\Delta S_{trans}$	$T\Delta S_{rot}$	$T\Delta S_{conf}$	$T\Delta S_{tot}$
	-40	-40	-	-80 least stable
	-24	-24	-10	-58
	-24	-24	0	-48 most stable

a) T = 300K. Values in kcal/mol.

Rotational entropy, S_{rot}, reflects the freedom of a particle to rotate in space. The magnitude of rotational entropy is proportional to both the molecular weight and dimensions of the ball. The

magnitudes of rotational and translational entropy are comparable for our molecules, and we can use equation 3 to estimate these values. The cost of bringing N balls together is estimated with

$$TS_{rot} = 3 + \ln(MW) \quad \text{(eq 3)}$$
$$T\Delta S_{rot} = 8(N-1) \quad \text{(eq 4)}$$

equation 4. The values relevant to **1**, **2**, and **3** are summarized in Table I.

Conformational entropy.[11] In the context of this paper, conformational entropy, S_{conf}, reflects the ability of a molecule or an aggregate to move its constituent parts with respect to each other (primarily though rotations of single bonds). One estimate of conformational entropy can be obtained by counting the number of bonds that are (or are close to) free two- or three-fold rotors in the molecule. Aggregate **3** has three fewer such bonds than does **2** and we hypothesize that this difference is the origin of the relatively high stability of **3**.

We are investigating a geometric formalism for counting rotors based on the volume of space that the "ball" can sweep. A *rigid* string (few free rotors) of a given length *l* only allows the

$$TS_{conf} = 0.6\ln V \quad \text{(eq 5)}$$

ball to sweep out a shell with radius *l*. A *flexible* string (many free rotors) allows the ball to sweep though a majority of the entire sphere of radius *l*. The values of S_{conf} estimated using equation 5 are shown in Table I (MW = 300, volume = 100 A^3).[12]

To examine the role of ΔS_{conf} in the systems that we have synthesized, we pursued a strategy in which the central hub and terminal melamine units were conserved, while the spokes were varied. Aromatic spacers and amide linkages in hub$(M)_3$ replace more freely rotating single bonds in flex$(M)_3$. The initial volume swept out by flex$(M)_3$ is much greater than that for hub$(M)_3$. The volumes swept out for both **2** and **3** are similar and smaller. Thus the change in accessible volumes upon aggregation is much greater for **2** than for **3**; this difference translates into a greater entropic cost of assembly for **2** than for **3**. Based on this simple model, we expect that the formation of **3** will be more favorable than **2**. Competition experiments monitored by ^1H NMR spectroscopy support this expectation of greater stability for **3** relative to **2**.

Computation

Computer simulations. The design of large aggregates can be made more efficient by using molecular mechanics and dynamics calculations. Two issues complicate this use. First,

molecular dynamics simulations are not appropriate (due primarily to limitations in computation speed and time) for sampling all of the relevant conformations of reactants, intermediates, and products that occur during the process of assembly of an aggregate. Equilibrium constants, therefore, are not available and a surrogate measure of stabilities must be developed. Second, the role of solvent in aggregates is critical; solvent must be incorporated into any calculation at some level.

Finding a surrogate for relative stablilities can be achieved by combining concepts from physical-organic chemistry with the tools of computational chemistry. We know, from the work of Cram[13] and others, that preorganization strongly influences strengths of binding in non-covalent compounds. This rationale is usually reserved for host-guest systems that have a structurally obvious "complementarity of fit." Unlike these systems, aggregates **1-3** are not highly preorganized for binding initially; they must adopt the appropiate conformation on aggregation. The "organization" in **2** and **3** entails: i) orienting the CA and M groups so that they form a planar rosette structure; and ii) minimizing the magnitude of oscillations from planarity of the CA and M groups in the rosette. Our goals in implementing molecular dynamics were to establish a method that provided a quantitative value--although not necessarily the value of free energy--related to the stability of the aggregate; and ii) to develop a rapid and accurate strategy for obtaining these values.

Procedure for the Construction of Aggregates. The initial conformation of the aggregates examined with molecular dynamics calculations was based on inferences from the ^{1}H and ^{13}C spectra of the aggregates in $CDCl_3$. The CA•M rosette was initially constrained to a planar geometry, and the arms of the trismelamines (of **2** and **3**) were attached to the rosette and rotated to preserve the C_3 symmetry observed in the ^{1}H and ^{13}C spectra. Amides were constrained to a *trans* configuration. The constraints were removed, and the potential energy of the aggregate was minimized. The resulting structure served as the starting point for further refinements and analyses using molecular dynamics.

Solvent plays a critical role in the structure of the modeled complexes. Minimizations of **3** with and without solvent gave drastically different results (Scheme 3). In the absence of solvent, the C_3 symmetry of the aggregate was destroyed as the rosette bowed inward to fill the empty central cavity. In the presence of solvent (84 molecules of $CHCl_3$), the rosette remained coplanar, and a molecule of solvent was confined within the central cavity of the aggregate. The structure incorporating a solvent molecule maintained the coplanarity of its CA_3·M_3 rosette throughout the minimizations and a 60 ps simulation. The three-fold symmetry of the complex inferred from ^{1}H NMR data was also maintained.

In the simulation of **3**•84$CHCl_3$, we observed that four molecules of chloroform are most strongly associated with the complex; the remaining molecules of solvent behaved as bulk solvent

and appeared not to interact strongly with the aggregate.[14] The results of a simulation with these four molecules of solvent suggested that the equilibrium geometries and dynamic behavior of **3**•4$CHCl_3$ and **3**•84$CHCl_3$ are very similar. This comparison, along with our desire to reduce computational times, provided the motivation to continue the simulations with the reduced system: (**2** or **3**)•4$CHCl_3$.

The deviation from planarity of the rosettes offers a quantitative metric for stability. The extent of the deviation from planarity (DP) of the rosette of an aggregate is easily measured in CHARMm by calculating the root mean square (RMS) deviation, in angstroms, between non-hydrogen atoms in the $CA_3 \cdot M_3$ rosette and a plane fitted to these atoms by a least-

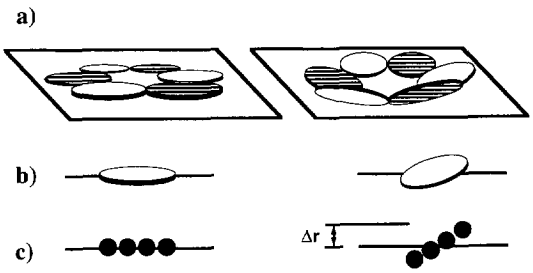

Scheme 3. The origin of the DP calculation for two rosettes of different shape. (a) The rosette on the left is flatter than the one on the right. It will have a smaller DP value and should be more stable. (b) To calculate DP, a plane is fit through the rosette. This plane is represented as a line. One melamine group is shown from each rosette for comparison. For a flat rosette, all atoms of the single disk are common to the plane. (c) The positions of the non-hydrogen atoms of the disks in (b) are shown as (•) and the distance Δr of each atom from the plane is calculated. For a flat rosette Δr = DP = 0. (d) The equation shown yields the DP value. N = the number of atoms.

squares method.[17] This calculation is represented pictorially in Scheme 3. The values of DP from the minimized structure and from the simulations for **1**, **2**, and **3** are shown in Table II.[15] Based on a limited data set, we suggest that the relative magnitudes of DP are inversely proportional to the relative experimental thermodynamic stabilities of the aggregates: that is, **3** has a smaller value of DP than **2** and is more stable.

Table II. Values of DP for Aggregates 1, 2, and 3.[15]

	DP	
	Minimization	**Dynamics**
	**0.5**	—
	**0.4**	**0.6**
	**0.3**	**0.5**

Conclusions

We are making progress toward our goal of the rational design of aggregates. This progress is a result of: i) a systematic program of synthesis, and evaluation of stabilities using physical-organic techniques; ii) the application of molecular mechanics and dynamics calculations to design and evaluate these aggregates prior to synthesis; and iii) an increasingly sophisticated understanding of the thermodynamic parameters governing aggregation. We have generated a series of aggregates that will serve as a basis set for refining theory and computation.

Experimental evidence indicates that solvent plays a critical role in the stability of these aggregates; this conclusion is supported by molecular mechanics and molecular dynamics calculations. The role of solvent remains to be incorporated fully in the theoretical model that we are developing. The theoretical model assumes that the enthalpies of formation of all of these aggregates are the same--a result of the conserved rosette motif. This assumption is not necessarily correct. It is unlikely that the equilibrium geometry of the CA and M groups are identical in different aggregates, and geometry influences the enthalpy of hydrogen bonds. Steric interactions between groups within the linker arms can also affect the total enthalpy of the system. The model does, however, offer a convenient starting point for the consideration of entropic components involved in association events, and yields estimates of these components.

Methods

Synthesis and characterization. The synthesis and characterization of **1**, **2**, and **3** have been reported.[4,5]

Molecular Modelling and Simulation. All simulations and energy calculations were done using the CHARMm program.[16] The parameters used in the calculations are from the CHARMm 22 force field.[17] We constructed the *neo*-hexyl isocyanurate and trismelamines using standard valence geometries, with the QUANTA 3.3 molecular modeling program.[18] Polar hydrogens were included and an extended atom representation was used for all non-polar alkyl groups. The melamine and isocyanurate groups of the complex were initially set to a planar geometry with a distance of 1.8 Å assigned to hydrogen bonds.[19] The complexes were assembled around the $CA_3 \cdot M_3$ rosette (Scheme I), and the torsional angles in the spokes of the tripods (excluding -CONH- torsional angles) were rotated so that the center of the tripod was at its maximum distance from the plane of the $CA_3 \cdot M_3$ rosette. The torsional angles were also rotated to maintain the average C_3 symmetry of the complexes inferred from NMR experiments. Energetically unfavorable steric interactions in the complexes were relaxed by performing 1000 steps of the Conjugate Gradient energy-minimizing algorithm; the resulting configurations served as the starting points for further structural refinements.

References

1. This work was supported by NSF grant CHE-19988321. M.M is an Eli Lilly Predoctoral Fellow (1993-). D.M.G. is an NIH Post-doctoral Fellow (1992-1994). J.P.M. was a SERC-NATO Post-doctoral Fellow (1991-1993). C.T.S. was an Eli Lilly Predoctoral Fellow (1991).

2. See, for example: Wyler, R.; de Mendoza, J.; Rebek, J. *Angew. Chem., Int. Ed. Eng.* **1993**, *32*, 1699. Geib, S.J.; Vicent, C.; Fan, E.; Hamilton, A.D. *Angew. Chem., Int. Ed. Eng.* **1993**, *32*, 80. Webb, T.H.; Suh, H.; Wilcox, C.S. *J. Am. Chem. Soc.* **1991**, *113*, 8554. Zimmerman, S.C.; Saionz, K.W.; Zeng, Z. *Proc. Natl. Acad. Sci. U.S.A.* **1993**, *90*, 1190.

3. Rosette in the solid state: Zerkowski, J. A.; Whitesides, G. M. *J. Am. Chem. Soc.* **1992**, *114*, 5473. Rosette in solution: Mathias, J. P.; Simanek, E. E.; Zerkowski, J. A.; Seto, C. T.; Whitesides, G. M. *J. Am. Chem. Soc.* **1994**, In Press. X-ray structure of CA•M: Wang, Y.; Wei, B.; Wang, Q. *J. Crystallogr. Spectroc. Res.* **1990**, 79.

4. See, ref 3. "Rosettes in the solution" for more details of this system.

5. Seto, C. T.; Whitesides, G. M. *J. Am. Chem. Soc.* **1993**, *115*, 905.

6. *Comprehensive Heterocyclic Chemistry*, J. M. E. Quirke, Pergamon Press, NY. 1984, vol 3, 157.

7. Davis, T. L.; Blanchard, K. C. *J. Am. Chem. Soc.* **1929**, *51*, 1801 and references therein.

8. Close, W. *J. Am. Chem. Soc.* **1953**, *75*, 3617.

9. *Organic Syntheses. Collective Volume II.* A.H. Blatt, ed., 1943, p 60. John Wiley & Sons. NY.

10. Solution corrections for the gas phase translational entropy calculated using the Sackur-Tetrode equation (*Statistical Mechanics*, D. A. McQuarrie. Harper and Row Publishers, NY. 1973, 86). employ an interpretaion of Trouton's rule for entropy of vaporization previously employed by Williams (Doig, A. J.; Williames D. H. *J. Am. Chem. Soc.* **1992**, *114*, 338-343).

11. True vibrational entropy--high freqency IR-active motions such as bond stretches and bends--contribute negligibly to the overall change in entropy. Go, N.; Scheraga, H.A. *Macromolecules*, **1976**, *9*, 535.

12. Unpublished results, Mammen, M.; Deutch, J.; Whitesides, G. M.

13. Cram, D. J. *Angew. Chem., Int. Ed. Eng.* **1988**, *27*, 1009.

14. The choice to represent only the four molecules of solvent explicitly is arbitrary, to some extent. The four molecules of chloroform were chosen since the energy of interaction with the aggregate of this set was significantly larger than that of other molecules of solvent.

15. The DP value for **1** was calculated using the crystal structure. It serves as only a reference point to a known, real structure.

16. Brooks, B. R.; Bruccoleri, R. E.; Olafson, B. D.; States, D. J.; Swaminathan, S.; Karplus, M. *J. Comp. Chem.* **1983**, *4*, 187.

17. *QUANTA Parameter Handbook*, MSI: Burlington, MA, USA, 1992.

18. QUANTA 3.3 molecular modelling program, MSI, 1992.

19. Pranata, J.; Wierschke, S. G.; Jorgenson, W. L. *J. Am. Chem. Soc.* **1991**, *113*, 2810.

(*Received* 5 *May* 1994)